Titel/Title: Auditory Display for Telerobotic Transnasal Surgery Using a Continuum Robot

Autor*innen/Author(s): Black, David; Lilge, Sven; Fellmann, Carolin; Reinschluessel, Anke; Kreuer, Lars; Nabavi, Arya; Hahn, Horst; Kikinis, Ron & Burgner-Kahrs, Jessica

Veröffentlichungsversion/Published version: Postprint

Publikationsform/Type of publication: Artikel/Aufsatz

Zusätzliche Informationen/Additional information:

Accepted for publication in Journal of Medical Robotics Research. Version of record: https://doi.org/10.1142/S2424905X19500041
Contact:
David Black, Medical Image Computing, University of Bremen, Jacobs University, Bremen,Fraunhofer Institute for Digital Medicine MEVIS, Bremen, Germany. Email Address: david.black@mevis.fraunhofer.de

Auditory Display for Telerobotic Transnasal Surgery Using a Continuum Robot

David Black[*,†,‡,**], Sven Lilge[§], Carolin Fellmann[§], Anke V. Reinschluessel[¶], Lars Kreuer[§], Arya Nabavi[‖], Horst K. Hahn[†,‡], Ron Kikinis[*,‡], Jessica Burgner-Kahrs[§]

[*]*Medical Image Computing, University of Bremen, Germany*

[†]*Jacobs University, Bremen, Germany*

[‡]*Fraunhofer Institute for Digital Medicine MEVIS, Bremen, Germany*

[§]*Laboratory for Continuum Robotics, Leibniz University Hanover, Germany*

[¶]*Digital Media Lab, University of Bremen, Germany*

[‖]*Neurosurgery Klinikum Nordstadt, KRH Hanover, Germany*

Tubular continuum robots can follow complex curvilinear paths to reach restricted areas within the body. Using teleoperation, these robots can help minimize incisions and reduce trauma. However, drawbacks include the lack of haptic feedback and a limited view of the situs, often due to camera occlusion. This work presents novel auditory display to enhance interaction with such continuum robots to increase accuracy and path-following efficiency and reduce cognitive workload. We recreate a typical use case with a test environment that simulates a transnasal intervention through the sphenoidal sinus including a simulated continuum robot. Distance information is mapped to changes in a real-time audio synthesizer using sung voice to provide navigation cues. User studies with novice participants and clinicians were performed to evaluate the effects of auditory display on accuracy, task time, path following efficiency, subjective workload, and usability. When using auditory display, participants exhibit significant increase in accuracy, efficiency, and task time compared to visual-only display. Auditory display reduced subjective workload and raised usefulness and satisfaction ratings. The addition of auditory display for augmenting interaction with a teleoperated continuum robot has shown to benefit performance as well as usability. The method could benefit other scenarios in navigated surgery to increase accuracy and reduce workload.

Keywords: Continuum robot; transnasal surgery; human–computer interaction; surgical navigation; sonification; auditory display; neurosurgery; user interfaces; usability; task load.

1. Introduction

Tubular continuum robots are characterized by their nonlinear shape and small diameter ($< 2.5\,\mathrm{mm}$). For medical interventions, this enables manipulation of the robots via nonlinear complex paths through natural orifices to restricted areas in the situs. These robots consist of biocompatible, flexible, pre-curved tubes nested into one other, which are specifically chosen to meet the application requirements and patient anatomy. These form the so-called backbone of the manipulator. For a thorough review of the current state of research of tubular continuum robots, please see [1]. These flexible robots are meant to be used with control via teleoperation in most minimally invasive applications by the surgeon, who manipulates a master input device [2, 3]. Using this

input method, the robot manipulator (slave) follows the commands of the master who interacts with the environment through the robot.

In general, teleoperated surgical robots can enhance, for instance, minimization of incisions and trauma as well as reduce the physical load on the surgeon to allow natural hand–eye coordination, motion scaling and high-end filtering of natural tremors [4]. Thanks to these characteristics, tubular continuum robots have been suggested for many different clinical and medical applications; for a general overview, please see [5]. For example, Burgner *et al.* proposed the use of tubular continuum robots for intracerebral hemorrhage evacuation [6]. Other proposed applications of tubular continuum robots include use in intracardiac [7] and neurosurgical [8] interventions, all of which benefit from the robot's dexterity and miniaturization to allow minimally invasive surgery. Furthermore, teleoperated tubular continuum robots have been explored in transnasal skull-base surgery scenarios [9]. In this case, a tubular continuum robot is deployed through the transnasal access in order to reach tumors located at the skull base. The curvilinear shape of the robot enhances tumor reachability compared to straight and rigid tools. In this paper, we will, as in other studies, concentrate on transnasal skull base surgery as a use case to evaluate our developed methods.

Despite the advantages of tubular continuum robots, there are still drawbacks with current approaches. In most cases, interventions are performed endoscopically, causing the surgeon to lose the natural feeling of the forces of interaction with tissue structures that are normally exerted during the procedure. Additional challenges of teleoperation using surgical continuum robots include a limited view of the surgical site, a lack of visual depth information: commonly available 3D endoscopes do not physically fit inside the central cavity of the innermost tube diameter of 0.2 to 2.5 mm. In addition, due to the decoupling of input to end-effector position, there is an increased cognitive load on the operator due to the manipulation of a curvilinear instrument. It is difficult to infer the robots end-effector position from the endoscopic two-dimensional image with occlusions and the complex shape of the robot. Because of this substantial decoupling, the interaction (including repeated re-clutching) is much more complex than that of, for instance, a computer mouse or joystick, where input motion is mapped to motion of the controlled device or pointer in a more straightforward fashion. Furthermore, when the view of the endoscope is obscured, for instance by blood, navigation becomes more difficult.

To overcome some of these challenges, this work proposes employing results from the growing field of auditory display to provide guidance information through a hitherto relatively free sense. So-called auditory displays maps changes in an underlying set of data to changes in sound synthesis parameters. A well-known example of an auditory display used to transmit motion changes can be heard in common automobile parking assistance systems: the distance of the front or rear of an automobile to a stationary object is mapped to the inter-onset time between tones, often culminating in a steady tone once the automobile reaches a defined distance to other parked automobiles or obstacles. In a similar fashion, auditory displays for medical guidance can be used to hear changes in these navigated instruments. In this case, changes in motion of a tracked continuum robot are mapped to changes in parameters of a real-time digital sound synthesizer.

The primary motivations for developing auditory display for medical robot guidance include increasing clinician's awareness of surrounding structures, replacing the diminished sense of touch and assisting clinicians in correctly interpreting and more accurately following navigation paths. Although examples of auditory display in medical navigation are scarce, methods have been evaluated for radio-frequency ablation [10], biopsy needle placement [11], temporal bone drilling [12], skull base surgery [13], soft tissue resection [14, 15] and telerobotic surgery [16]. Previous evaluations of auditory displays for medical navigation have shown benefits including enhanced recognition of the distance to structures or targets, improved placement accuracy, reduced cognitive workload and reduced rates of clinical complication. Drawbacks reported in the literature include increased task completion time and increased nontarget tissue removed during resection. For a comprehensive review of auditory display in image-guided interventions, see Black *et al.* [17].

Previous work on teleoperation algorithms to assist continuum and surgical robots have focused on either automating several subtasks of teleoperation, such as obstacle avoidance, or providing the master with additional feedback for further support. For example, Leibrandt *et al.* [3] applied virtual fixtures to concentric-tube continuum robots. They proposed teleoperation algorithms that guide the user along stable and collision-free paths using haptic feedback. Kreuer *et al.* [18] implemented and evaluated a similar approach using a simulated transnasal endoscopic surgical intervention. Results have shown that in comparison with purely visual feedback, haptic feedback generated using virtual fixtures enables more intuitive teleoperation while also lowering the completion time of the presented tasks. Apart from providing additional feedback, some algorithms for teleoperation assistance also directly affect the motion generation of the continuum robot. For example, Torres *et al.* [19] proposed a system for concentric-tube continuum robots that allows teleoperation of the robot's

tip while helping avoid collisions along the robot's entire backbone. Furthermore, Gras *et al.* [20] have shown that an adaptive motion scaling during teleoperation of surgical robots can lead to more intuitive teleoperation due to less reliance on the 'clutch-in' mechanism. Medical needle guidance tasks have also been supported by haptic feedback with results from Culbertson *et al.* [21] showing decreased probe deviation and correction time, although Abayazid *et al.* [22] show similar accuracy and task completion time results for both haptic and visual feedback. It has been suggested that for enhancing motor learning, the use of auditory display compared to haptic feedback exhibits improved effectiveness for movement control and positioning [23]. Thus, the novelty and salience of both auditory display as well as teleoperated continuum robots make a combination of the two an ideal candidate for investigation.

This work describes a method to harness the benefits of auditory display to augment the task of virtual tubular continuum robot placement using a haptic input device. Tasks include (1) locating waypoint spheres inside a transnasal access passage and (2) avoiding the passage's walls. These two tasks are evaluated in a user study to compare the quantitative and qualitative benefits of using such a system with and without auditory display. In many clinical scenarios, image guidance navigation assistance for a tracked instrument can be given using three parameters: horizontal distance (left and right), vertical distance (up or down) and depth. This can be applied, for instance, to needle placement [24], image-guided laparoscopy [25], or transnasal telerobotics [6], where an instrument must be navigated to remain on the origin of a plane orthogonal to the line of a planned target. Thus, similar to navigation inside a tunnel, the instrument must remain along a trajectory until the target in depth has been reached. To the authors' knowledge, no auditory display has been explored yet for applications involving medical tubular continuum robot navigation. Thus, this work goes beyond the state of the art to increase the understanding of the role audio can play in hybrid-display clinical navigation systems, especially those in which tunnel-like scenarios play a large role. We hypothesize that the addition of auditory display will increase accuracy, efficiency and usability of continuum robot navigation as well as reduce cognitive workload for a task involving continuum robot navigation. We acknowledge that a simulated environment does not represent all of the many aspects that are present when dealing with a physical robotic system. Nevertheless, we evaluated the implemented novel auditory display methods in a simulated environment that represents many of the important aspects of continuum robot kinematics. The results of this evaluation are a first step towards the investigation of auditory displays for continuum robot teleoperation.

2. Methods

In this work, changes in motion of an input device controlled by the operator are applied to the end effector of a virtual tubular continuum robot composed of three tubes. The movement of the robot end effector is transmitted to a auditory display synthesizer, which produces auditory feedback to inform the operator about the continuum robot's location within the simulated environment.

2.1. *Robot system*

Each tube of the simulated tubular continuum robot in the virtual environment has two degrees of freedom. Typically, these robots are composed of three tubes, such that a configuration $\boldsymbol{q}$ consists of translational $[\beta_1, \beta_2, \beta_3]$ and rotational parameters $[\alpha_1, \alpha_2, \alpha_3]$. The quasi-statics mechanics-based model of the robot is based on [26]. The model determines the solution to the forward kinematics for a given configuration $\boldsymbol{q}$ as a continuous 3D curve describing the shape of the robot in terms of its centerline. In addition, the model is used to determine the manipulator's Jacobian $\boldsymbol{J}$. The kinematics model is based on the specific case of Kirchhoff of the Cosserat rod theory and may involve forces acting on the robot.

The input device (Geomagic Touch, 3D Systems [27]) is an impedance-controlled input device consisting of six degrees of freedom. It is controlled by a hand-held pen stylus for which the position and orientation in Cartesian space are detected at the pen tip. Velocity is calculated from the generated change in position of the pen tip to the desired end effector. Due to different workspaces of the input device and of the robot, a so-called 'clutch-in' mechanism is applied by pressing a button on the stylus to move the end effector of the robot. By releasing this button, the stylus can be repositioned without end-effector movement.

The motion of the input device commanded by the operator is expressed as a desired end-effector velocity $\dot{\boldsymbol{x}}_{\text{des}}$ (position and angular velocity) dependent on the current simulated continuum robot pose $\boldsymbol{x}_{\text{robot}}$, which is obtained using the kinematic model description described in [26]. Then, the pseudoinverse of the manipulator Jacobian matrix $\boldsymbol{J}^{\dagger}$ is used to calculate the corresponding joint velocities $\dot{\boldsymbol{q}}$ [28]. These are summed up to the current joint values $\boldsymbol{q}$ of the simulated robot to move towards the desired position $\boldsymbol{x}_{\text{des}}$ and to update the end-effector position prediction based on the kinematic model. This process is shown in Fig. 1.

2.2. *Simulation environment and task description*

The simulation environment includes a virtual anatomical model of the transnasal access which was manually

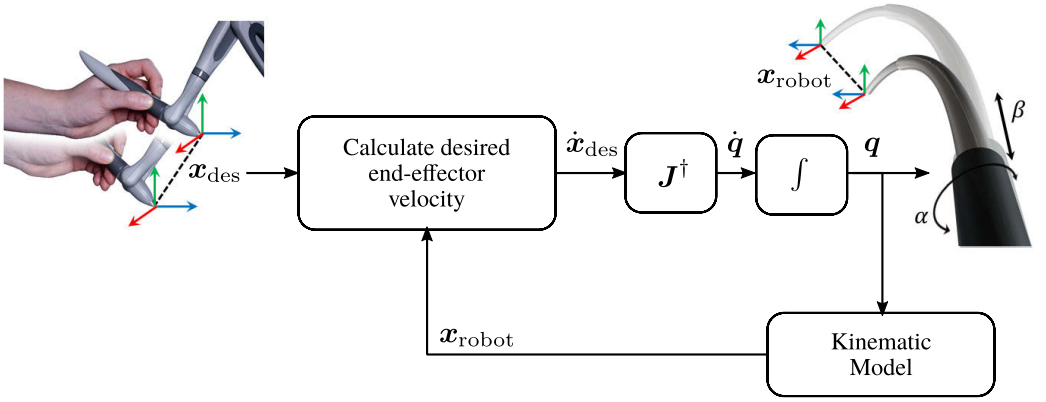

Fig. 1. Approach for teleoperation of tubular continuum robots.

segmented from a computed-tomography (CT) dataset of an adult skull base surgery patient. In the implemented scenario, the robot's end effector should be teleoperated through the transnasal access to the sphenoid sinus. This allows the manipulator to reach the patient's skull base, which is a common location of pituitary tumors.

For the implemented teleoperation environment, we chose a motion scaling factor of 0.1, resulting in a robot end-effector movement 10 times smaller than the movement at the input device (i.e. moving the input device by 1 cm leads to a end-effector movement of 1 mm). A visualization of both the robot and the anatomical model can be seen in Fig. 2. The camera view within this simulation mimics the camera view of an endoscope, which is typically guided alongside the robot through the transnasal access.

During robot teleoperation, we consider two different use cases. For the first, a path from the entrance of the transnasal access to the sphenoid sinus consisting of several discrete waypoints (in Fig. 2 shown as blue spheres). This path can be precomputed by a motion planning algorithm and serves as guidance for the teleoperating user, who steers the robot's end effector to each waypoint successively until the final waypoint has been reached. The second use case does not feature waypoints. For this task, the user navigates the robot's end effector towards the end of the transnasal corridor while avoiding collision with the walls of the anatomical model.

For both use cases, we propose that auditory display could assist the user in navigation in addition to the visual display of the simulation environment. For the use case of navigating waypoint spheres, the distances in the x- and y-directions between the robot's end effector and the next waypoint sphere with respect to the current virtual camera reference frame, and thus parallel to the image plane are calculated at every step of the teleoperation algorithm (see Fig. 3, left). In addition, the depth between the next waypoint and the robot's end effector is calculated using the same reference frame, resulting in an orthogonal vector to the image plane.

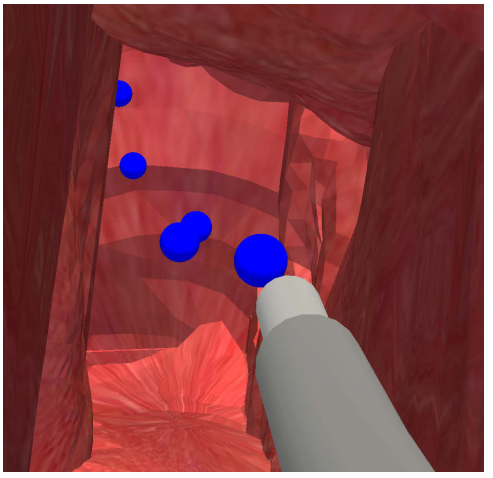

Fig. 2. Visualization of the implemented simulation environment depicting the robot (in gray), the virtual anatomical model (in dark red) and predefined spheres (blue) which serve as waypoints for navigation guidance.

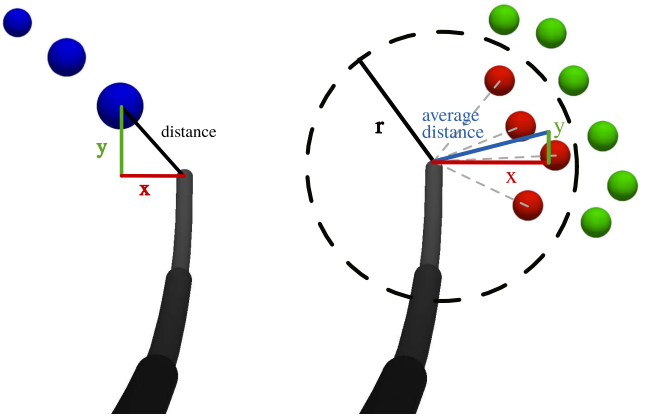

Fig. 3. Left: Calculation of the x and y distances between the next blue waypoint spheres of the path and the robot's end effector. Right: Radius search around the robot's end effector to find nearby anatomical data points (simplified as dots). Dots inside a specific radius r (marked in red) are averaged to calculate the x and y distances to the anatomical model.

For the use case of collision avoidance, the discrete data points of the virtual anatomic model are stored in an octree structure. This search tree structure can query collisions and distance checks based on the Euclidean distance between the queried point and the data points stored within this tree [29]. Using this octree, a radius search around the robot's end effector is performed at every step to find nearby anatomical data points. The x- and y-distances of the anatomy with respect to the robot's end effector are calculated by averaging the distances of all found data points within a specified radius (see Fig. 3, right). For this implementation, we chose 3.5 mm as radius. A distance between the robot and the anatomy greater than this specified radius can be considered as safe in the context of this application.

2.3. *Auditory display method for robot navigation*

For each of the two calculated metrics, the x- and y-distances to the next waypoint sphere (in mm) or the x- and y-distance (in mm) to the closest wall, an auditory display was developed to guide the user during both teleoperation use cases. The general approach for developing an auditory display for the continuum robot is based on mapping the three degrees of freedom in manipulator end-effector position to sound: horizontal distance from −10 mm (left) to +10 mm (right), vertical distance from −10 mm (below) to +10 mm (above), and depth (15 mm away from target to 0 mm at target). Throughout this work, no feedback based on the orientation of the manipulator is given, as the task only requires position control.

The auditory display method was developed using the PureData [30] visual music and sound programming environment. The development of the auditory display followed an iterative design process that included multiple rounds of hands-on preliminary evaluation with novice and expert users. In these preliminary iterations, some participants were irritated by purely synthesized 'electronic sounds', such as those similar to methods developed in previous studies (e.g. [10]), and thus, an improved method was developed to reduce unnecessary additional cognitive load resulting from annoyance. The subsequently developed and evaluated auditory display method described here employs a set of recorded samples of vocal singing to provide navigation cues. A 'vocal syllable choir' synthesizer responds to the end-effector position. Deviations from planned vertical distance, horizontal distance and depth are mapped to parameters of the auditory display synthesizer. The synthesizer harnesses pitch, syllable type and voice gender (for vertical distance mapping), stereo position (for horizontal distance mapping) and reverberation amount and inter-onset interval (for depth mapping), see Fig. 4 for a simplified representation of employed mappings.

Deviations in vertical distance are mapped to the pitch, syllable type and gender of the sung syllables for redundant cognition. Categories of syllables were first created for which sung syllable samples were recorded. This harnesses the powerful ability of humans to recognize syllables. The categories of syllables included [o:] for deviations *above* the x-axis (German: *oben*), [u:] (German: *unten*) for deviations *below* the x-axis trajectory, and hummed [m] when vertical distance was correct within a defined margin to create a steady confirmation tone. Pitches for deviations of the end effector below the x-axis range from E2 (82.41 Hz) at −10 mm to C3 (130.81 Hz) at −1.1 mm. Pitches for deviations above the x-axis range from C4 (261.63 Hz) at 1.1 mm to B4 (493.88 Hz) at 10 mm. For deviations within the defined margin ('correct vertical distance') deviations between −1 mm and 1 mm, a triad with hummed pitches E3-G3-A3 (164.81/196.00/440.00 Hz) is played.

Deviations in horizontal distance from the center are mapped to the stereo position of the output. In pilot studies as well as previous work [10], this was found to be an effective way of transmitting current horizontal distance compared to monaural presentation. Thus,

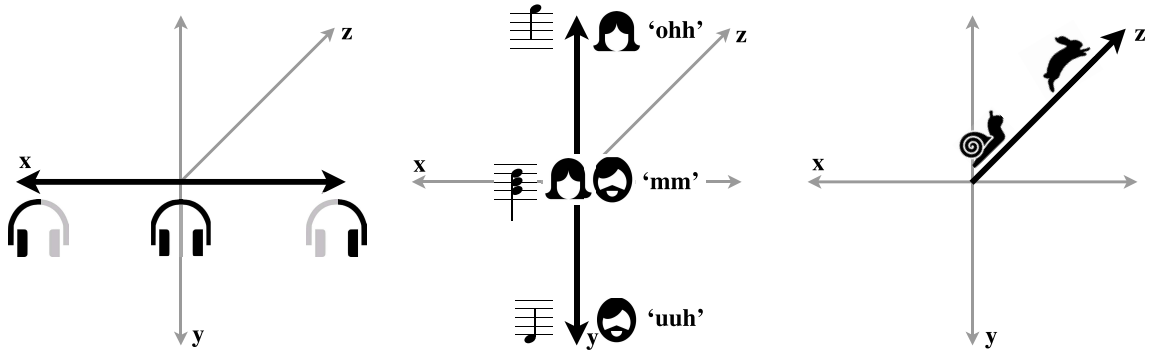

(a) horizontal distance (b) vertical distance (c) depth

Fig. 4. Primary auditory display mappings: Horizontal distance (a) from center is mapped to stereo panning. Vertical distance (b) is mapped to pitch, sung syllable and sung gender type. Depth (c) is mapped to inter-onset interval of sung syllable samples.

when the tip of the robot is located to the left of the center, sound output is heard in the left ear. When the tip is located to the right of the center, sound output is heard in the right ear. Between −1 mm and 1 mm, output is heard with a linear amplitude mapping between left and right ears. Outside this distance, the output is heard completely in the left or right ear to aid discrimination and enhance fine horizonal adjustment near the center.

For the waypoint navigation task, deviations in depth are mapped to the inter-onset interval of the sung samples as well as the amount of reverberation mix. At the furthest distance (15 mm) to the next sphere, the inter-onset interval is 450 ms, which increases to 250 ms when at the sphere. Because each sung syllable sample is approximately 1 second in duration, samples are overlapped, creating a choir effect with up to 8 samples played back at once. The amount of reverberation mix (using the freeverb~ [31] object) is 30% at the furthest depth (15 mm) and 0% when at the target sphere. The overall resultant sound is that of a medium-sized choir with the ability to represent changes in horizontal distance, vertical distance and depth.

2.4. *Experimental design*

We conducted evaluations on the effect of auditory display as augmentation for navigating a virtual tubular continuum robot through the sphenoidal sinus to the pituitary gland. We completed two user studies: the first with a group of students and scientific personnel recruited from the local university, and the second with clinicians that featured a smaller set of tasks. Compared to visual display, we hypothesized that using the auditory display will:

(H1) increase *accuracy* during navigation
(H2) increase task completion *time*[a]
(H3) increase path following *efficiency*
(H4) reduce overall *task load*
(H5) increase overall *usability*.

The two conditions differed only in the presentation of navigational information:

(V) only *visual* display on the screen
(A) additional *auditory* display.

We employed a within-subject design and controlled for potential learning effects by using a Latin-square scheme for the order of conditions and tasks. Based on the two aforementioned scenarios of teleoperational sphenoidal sinus surgery, the two tasks included:

(N) *Navigation* of waypoint spheres in sphen. sinus
(C) *Collision avoidance* of passage walls.

[a] An increase in task completion time has been observed in previous approaches (e.g. [10, 14, 17]), such that we also predict such an increase.

This resulted in four task/condition combinations: NV (navigation with visual display), NA (navigation with auditory display), CV (collision avoidance with visual display) and CA (collision avoidance with auditory display).

During task execution, we recorded the position of the robot's end effector, the position of the nearest anatomy with respect to the robot's end effector as well as the corresponding Euclidean distance between them. We calculated accuracy of the tip, path efficiency and task completion time. A questionnaire provided insight into perceived workload, system acceptance with regards to usefulness and satisfaction and participant agreement with confidence, ease of use, time needed and helpfulness of each task/condition combination. In addition, we asked the participants to rank the overall usability of each of the task/condition combinations.

The waypoint navigation (NV and NA) task consisted of guiding the robot along a route delineated by six blue spheres. For this task, participants were instructed to navigate the robot towards and hit the center of each sphere. Accuracy was measured as the Euclidean distance of the end effector to the center of the blue sphere when passing it. Task completion time was determined by the elapsed time between the moments the participant crossed one blue sphere to the consecutive sphere. An efficiency score based on ISO/IEC 9126-4 ([32]) was calculated based on the accuracy and task completion time as t/dev^2 where dev is the deviation as the absolute distance from the tip of the robot to the sphere when passed, and t is task completion time, the elapsed duration needed between two consecutive spheres. This appropriately weights the accuracy higher than the task time which was chosen based on discussions with collaborating clinicians. Alternating spheres were occluded by simulated blood to create an obstacle that might occur in a real operating situation. To visualize this, a large red sphere appears for every second sphere that restricts the line of sight. This should allow a comparison of performance between visible and hidden spheres to determine how well the auditory feedback can guide a user with and without visual assistance.

The collision avoidance (CV and CA) task consisted of guiding the robot through a tunnel without colliding with the walls, which represented fragile structures in the sphenoidal sinus. Similar to the navigation task, simulated blood was displayed in the 3D environment. Accuracy was determined as the average distance to the walls of the anatomical sphenoidal sinus model. Task completion time was determined by the time needed to proceed through the entire transnasal corridor.

2.5. *Evaluation procedure*

The studies took place in an enclosed laboratory. The test workstation consisted of a computer with a 24 inch monitor and a Geomagic Touch input device [27].

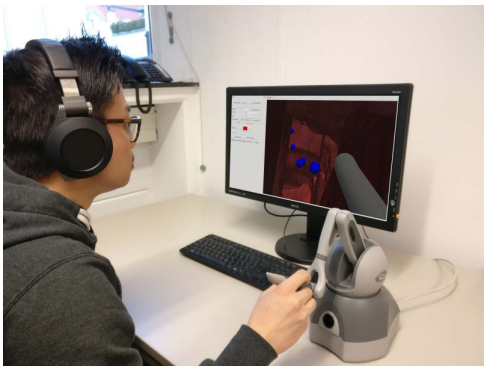

Fig. 5. Evaluation setup with Geomagic touch input device.

Over-ear studio headphones were provided for each participant. Participants were visually separated from each other and were seated during the entire evaluation procedure. Participants were permitted to adjust chair and input device position and rest their arm on the testing table.

Participants received a 5-minute tutorial video and a 1-page explanation two days before the study to familiarize themselves with the study tasks and the auditory display methods. After providing informed consent, the participants were assigned, according to the Latin-square counterbalance scheme, to one of the tasks and conditions to begin. The evaluation was conducted using the aforementioned tasks. Before each task/condition combination, the participants received 5-min task-specific training and performed a single training run. Participants were instructed to complete all tasks as quickly and accurately as possible, thereby determining their own balance between time and accuracy.

After completing each of the four task/condition combinations, the participants completed a questionnaire about their experience. The questionnaire included NASA TLX [33], which measures the cognitive workload experienced by the participants while completing the task. We employed the Raw TLX scale, as the weighted scale involves a greater amount of time for the participant to complete and has not been conclusively shown to produce extra benefits [34]. In addition, the commonly employed van der Laan Technology Acceptance Scale [35] was provided to evaluate the usefulness of and satisfaction with using the teleoperation system with each of the task/condition combinations. This scale includes nine pairs of adjectives, such as “undesirable/desirable” or “nice/annoying” to generate composite ratings for usefulness and satisfaction. Finally, four questions were asked concerning participants’ agreement with confidence in executing the task, ease of use of the method, satisfaction with the time needed to complete the tasks and helpfulness of the display method. At the conclusion of the study, the participants completed a questionnaire concerning demographics (age, handedness, visual and hearing impairments, video gaming frequency) as well as a single ranking of the participant’s preference for each of the task/condition combinations.

2.6. *Statistical analysis*

The data was analyzed using R [36]. All data gathered from Study 1, including task completion time, accuracy, efficiency, NASA TLX score and van der Laan scores were analyzed with the nonparametric Wilcoxon signed-rank test. These nonparametric tests require less assumptions and hence are more robust in the case of small sample sizes as used in our paper [38]. The level of significance, i.e. the statistical difference of the means, was indicated by $p < 0.05$. For study 2, we did not perform an inferential statistical analysis, as the sample size was too small to gain meaningful outcomes in terms of significance. Therefore, we present averages and box-and-whisker plots as a descriptive approach to show the magnitude of the effects.

3. Results

Study 1 was completed by 16 novice participants. The participants had an average age of 28.1 (ranging from 23 to 31). The participants were students recruited from Leibniz University in Hanover, Germany, and all had a background in scientific fields of study. Eight wore corrective lenses. None of the participants stated any limitations regarding their hearing abilities. One of the participants was left-handed but performed the evaluation with the right hand; the remaining were right-handed. Asked about their gaming frequency, 31% (5) of the participants stated that they game about once per month, 24% (4) weekly, 19% (3) a few times a year, and 25% (4) less than once a year.

Study 2 was completed by five clinical participants. The participants had an average age of 32.2 (ranging from 19 to 51), with 1 female and 4 males. The participants were recruited from the International Neuroscience Institute in Hanover, Germany. Four were neurosurgeons and one was a medical student. All wore corrective lenses. None of the participants stated any limitations regarding their hearing abilities. All participants were right-handed. Asked about their gaming frequency, 20% (1) of the participants stated that they game a few times a week, while 80% (4) play less than once a year. Due to the lack of significant results from Study 1 as well as resource constraints, we elected not to perform the collision tasks (CA and CV) with clinicians.

3.1. *Accuracy*

Study 1. For the waypoint navigation task, the average absolute distance (error) in the x–y plane of the end

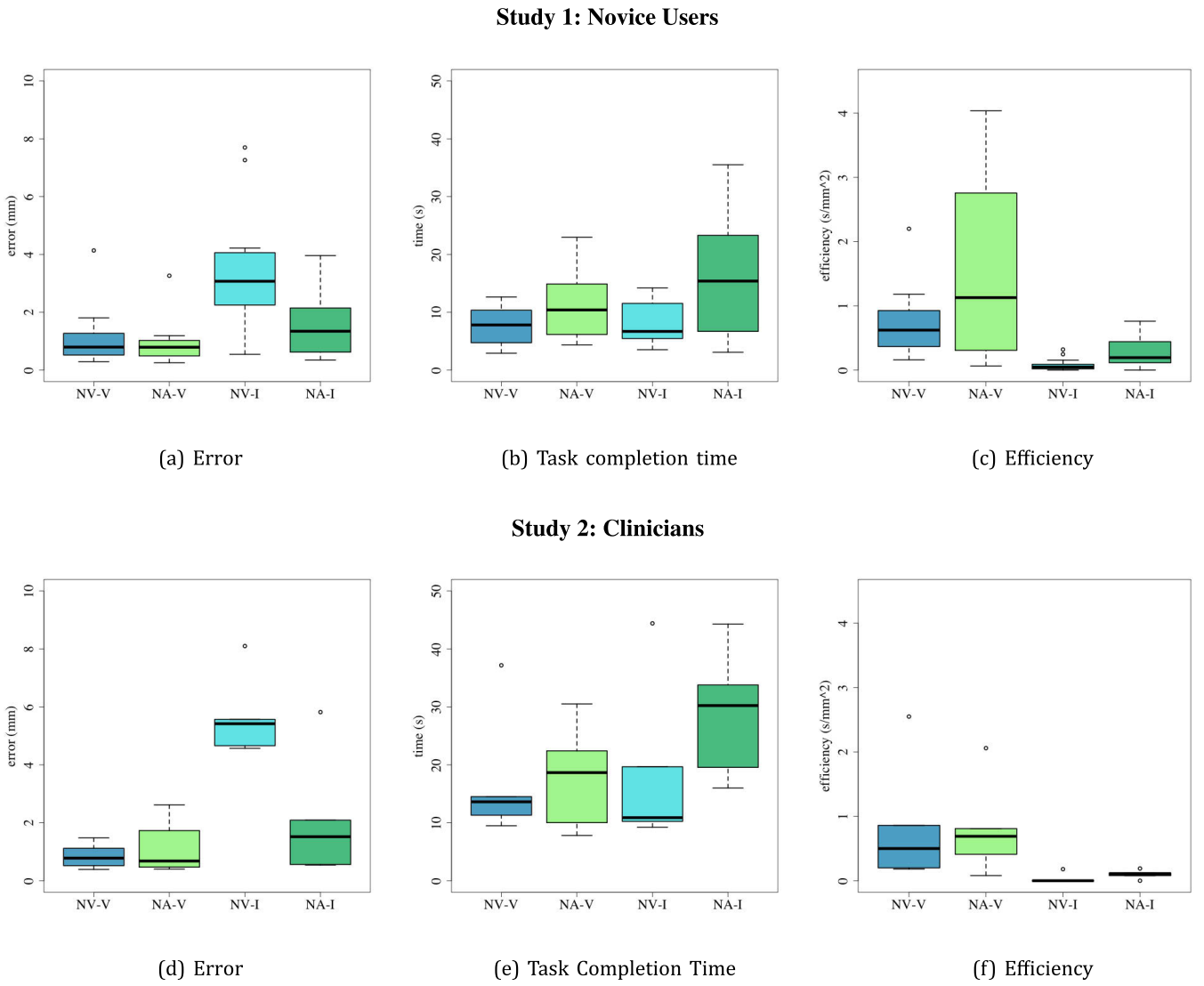

Fig. 6. Average error (in mm), task completion time (in s), and efficiency (s/mm^2) per sphere during the waypoint navigation task, where NV-V and NA-V indicate visual and auditory display for visible spheres, and NV-I and NA-I for invisible spheres.

effector to the passed sphere was measured in millimeters. Participants performed with significantly less error using auditory display (NA) compared to visual display (NV), see Fig. 6(a). For visible spheres, the average error was 1.08 mm using visual display and 0.89 mm using auditory display. For hidden spheres, the average error was 3.43 mm using visual display and 1.49 mm using auditory display. For the collision avoidance task, the average distance to the anatomical model was similar for both conditions: 3.00 mm for visual display and 2.97 mm for auditory display, although this did not reach a level of significance.

Study 2. Participants in Study 2 performed similarly to those in Study 1, see Fig. 6(d). For visible spheres, the average error was 0.92 mm using visual display and 1.04 mm using auditory display. For hidden spheres, the average error using visual display 5.66 mm and 2.11 mm using auditory display.

3.2. *Task completion time*

Study 1. For the navigation task, the average time to hit each sphere was measured in seconds, with participants needing significantly longer using auditory display (NA) compared to visual display (NV), see Fig. 6(b). For visible spheres, the average task completion time per sphere was 7.60 s using visual display and 11.21 s using auditory display. For hidden spheres, the average completion time per sphere was 8.03 s using visual display and 15.57 s using auditory display. For the collision avoidance task, the task completion time was longer using auditory display (CA), with an average of 79.94 s than visual display (CV) with an average of 61.08 s, but did not reach a level of significance.

Study 2. For the waypoint navigation task (see Fig. 6(e)), the average task completion time per visible sphere was 17.39 s using visual display and 18.54 s using

auditory display. For hidden spheres, the average completion time per sphere was 18.89 s using visual display and 28.78 s using auditory display.

3.3. *Efficiency*

Study 1. Participants performed with significantly more efficiency using auditory display compared to visual display when approaching hidden spheres, see Fig. 6(c). For these spheres, the average efficiency time per sphere in s/mm^2 was 0.08 using visual display and 0.28 using auditory display. For visible spheres, the average efficiency per sphere was 0.72 using visual display and 2.20 using auditory display, although a level of significance could not be reached.

Study 2. Clinical participants in Study 2 performed more efficiently using auditory display compared to visual display when approaching hidden spheres, see Fig. 6(f). For visible spheres, the average efficiency per sphere was almost equal using both visual and auditory display.

3.4. *Subjective workload*

Task load was calculated as the overall task load index according to the NASA Raw TLX questionnaire [33, 34], the results of which are presented in Figs. 7(a) and 7(d). The subjective workload is presented as an overall scores ranging from 0 (best) to 100 (worst). In Study 1, for both navigation and collision tasks, using the auditory display

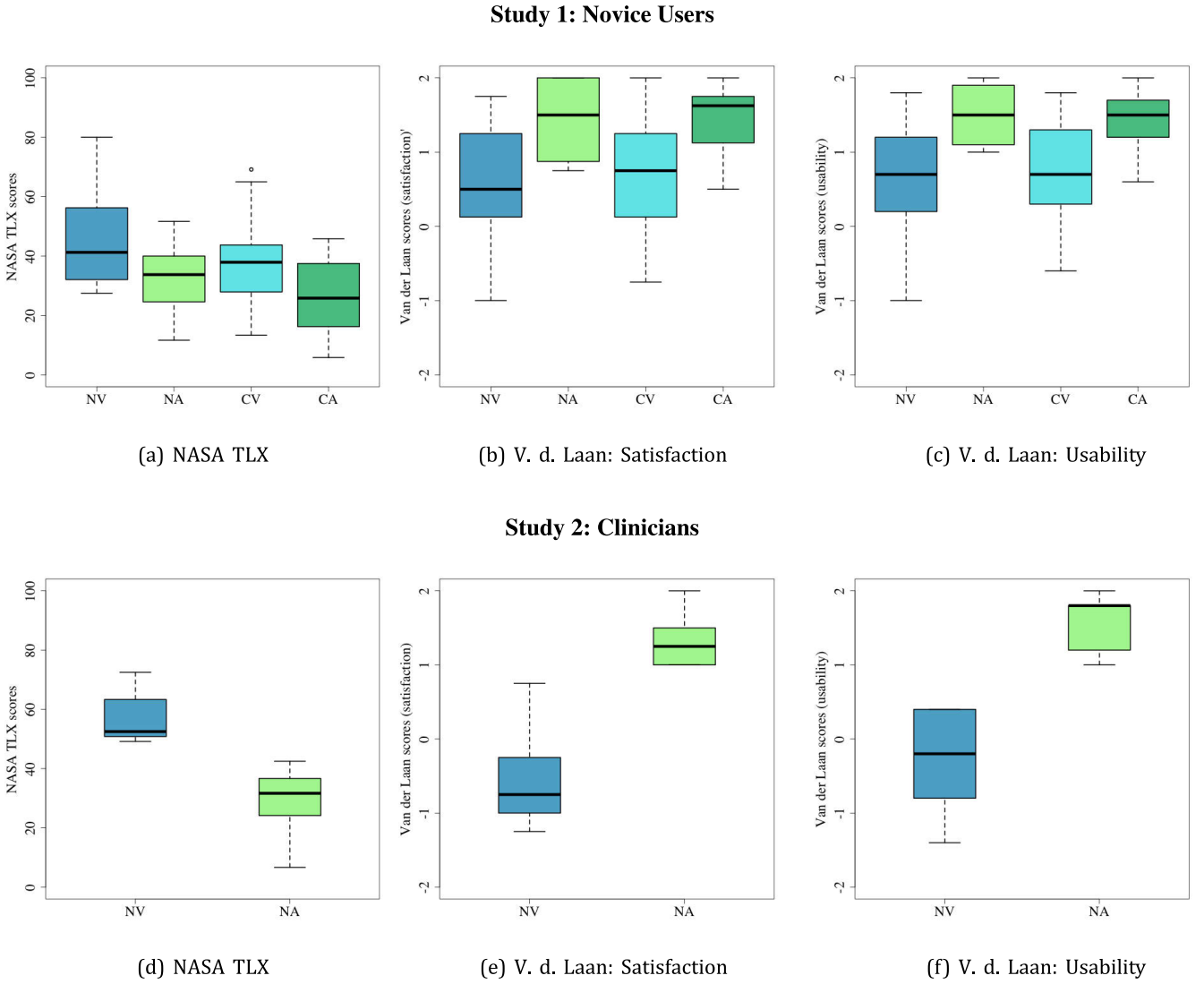

(a) NASA TLX (b) V. d. Laan: Satisfaction (c) V. d. Laan: Usability

(d) NASA TLX (e) V. d. Laan: Satisfaction (f) V. d. Laan: Usability

Fig. 7. Questionnaire scores for waypoint navigation task for visual (NV) and auditory display (NA) and collision avoidance for visual (CV) and auditory (CA) display. Ranges for NASA Raw TLX are 0 (low workload) to 100 (high workload) and for van der Laan from −2 (fully reject) to 2 (fully accept).

was rated with significantly lower overall subjective workload than using only the visual display. In addition, for every dimension of the index and for each task, the auditory display was rated with significantly lower subjective workload. In Study 2, using auditory display was rated with lower overall subjective load than with visual display.

3.5. *System acceptance*

Figures 7(b), 7(c), 7(e) and 7(f) present the results of the van der Laan system acceptance questionnaire [35] as both composite *usefulness* and *satisfying* scales, with combined scores ranging from −2 (fully reject) to 2 (fully accept). In Study 1, for both tasks, both the usefulness as well as satisfaction when using auditory display were rated as significantly higher than when using visual display. In Study 2, both the usefulness as well as satisfaction when using auditory display were rated higher than when using visual display.

3.6. *Participant agreement*

The results of participant satisfaction with confidence during use, ease of use, time needed to complete the tasks, and helpfulness of the display are shown in Table 1, with scores on a 7-point Likert scale ranging from 1 (complete agreement) to 7 (complete disagreement). For Study 1, for both navigation and collision avoidance tasks, using auditory display was rated as providing significantly higher satisfaction in all measures. For Study 2, all participants rated auditory display higher than visual display for the waypoint navigation task.

3.7. *Overall ranking*

For Study 1, participants were asked at the end of completing all tasks to assign an overall rank of each of the four task/condition combinations from least to most preferred, receiving 0–3 points. The average rating scores for each combination are shown in Fig. 8.

Table 1. Mean values for agreement questionnaire results for all conditions, ranging from 1 (strongly agree) to 7 (strongly disagree).

	Study 1				Study 2	
Measure	NV	NA	CV	CA	NV	NA
Confidence	3.88	2.13	2.75	1.94	6.00	2.00
Ease of use	3.12	1.81	2.56	1.80	5.40	2.00
Time needed	2.38	2.00	2.38	1.81	3.20	2.20
Helpfulness	4.50	1.81	4.63	1.75	5.75	1.40
Average	**3.47**	**1.94**	**3.08**	**1.83**	**5.09**	**1.90**

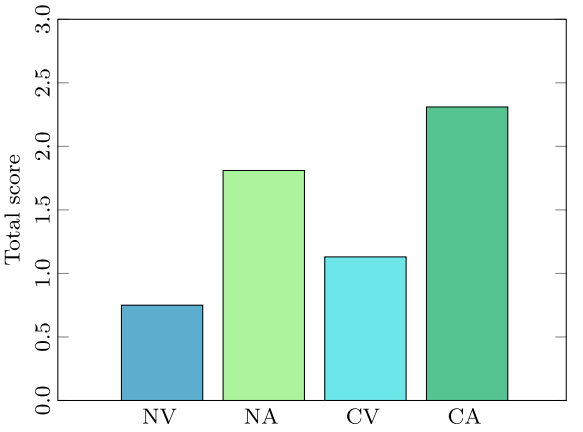

Fig. 8. Average overall ranking scores for each task/condition combination for Study 1, from 0 (least preferred) to 3 (most preferred).

CA was preferred the most with an average rank of 2.31, NA with an average of 1.81, CV with an average of 1.13 and NV with an average of 0.75. For Study 2, participants ranked only NV and NA, and all five preferred NA.

4. Discussion

For the waypoint navigation task (N), results of the user study confirm all of our hypotheses. In Study 1, accuracy (H1) in hitting waypoint spheres was significantly improved using auditory display (NA) over visual display (NV), showing that the auditory display provides exceptional performance benefit in accuracy not only when the user cannot see the target on the screen, but also during navigation of visible spheres. Interestingly, in Study 1, average accuracy for invisible spheres was even higher using auditory display than for visible spheres using visual display. Accuracy in path following is important because critical structures should be hit as little as possible. The calculation of accuracy by means of a waypoint task helps recreate the medical scenario in which the walls of the transnasal corridor should not be hit.

Our hypothesis for task completion time (H2) was also confirmed; the tasks took significantly longer using auditory display than with visual display. This was expected, considering similar results in the literature [10, 14, 17] have shown that performance with the addition of auditory display entails significantly more time. During post-experimental discussions with study participants, we received feedback that this could be due to the novelty of the introduced method: many users are already familiar with visual displays, spending hours interacting, for instance, with mouse and cursor on a

computer screen) but less so with auditory displays, where the most typical interaction might be car parking aids, which are used, at most, a few seconds per day. Although accuracy results were similar between both Study 1 and Study 2, task completion time for Study 2 was higher for all conditions, although relative times between conditions were similar to those in Study 1, see Fig. 6. This is most likely due to the fact that clinicians placed more emphasis on accuracy at the expense of longer task time.

Our hypothesis concerning efficiency in path following (H3) was partially confirmed; auditory display provided significant increases in efficiency for invisible spheres and non-significant increases for visible spheres.

For all measures gathered using the questionnaire (NASA TLX Workload, van der Laan system acceptance, and agreement with confidence, ease, time and helpfulness), auditory display provided significantly improved scores, thus confirming both H4 (reduce overall task load) and H5 (increase usability). Mean values for both overall workload and system acceptance as well as all individual factors showed that the auditory display improved interaction. In addition, using auditory display for waypoint navigation was ranked higher overall than visual display by 12 of the 16 participants. The group of physicians in Study 2 exhibited similar performance to novice participants in Study 1, although average task time was higher.

For clinical participants, the difference in subjective measures (NASA TLX, van der Laan and agreement questionnaires) between auditory and visual displays were much greater for all scales than participants in Study 1.

For the collision avoidance task (CV and CA) performed only in Study 1, significant differences were not found in either the task completion time or accuracy. Thus, we are unable to confirm H1 and H2 for this task. These results might be due to the setup environment of the collision avoidance task, as all participants were able to complete the task without any great difficulty. However, using auditory display was shown to provide significant benefits with respect to both overall NASA TLX subjective workload and van der Laan scale in both usefulness and satisfying scales, confirming H4 and H5. In addition, 13 of the 16 participants in Study 1 ranked the interaction with the auditory display for the collision avoidance task higher than interaction with visual display. These results indicate that despite the lack of significant performance improvements in accuracy or task completion time, the auditory display created a more agreeable means of robot interaction and was preferred by most participants. Due to the lack of significant results from Study 1, we elected not to perform the collision tasks (CA and CV) with clinicians, due to time and resource constraints.

Overall, we confirm the hypothesized benefits of using auditory display for supporting interaction with a continuum robot for the virtual sphenoidal sinus intervention scenario. Although participants only completed a brief, 5-minute training phase, the auditory method has been shown to benefit a task that is hitherto performed with only visual display. It has been demonstrated to provide completely 'blind' (screen-free) instrument placement, as well as to increase accuracy and efficiency as well as decrease subjective workload and improve satisfaction. The auditory display also helped improve interaction even when significant performance benefits were not exhibited such as during the collision avoidance task. Although task times were, as hypothesized, longer when using auditory display, we believe that with increased training with and exposure to this method and auditory displays in general, task completion time could be reduced.

The differences between the results of Study 1 and Study 2 were pronounced, whereas novice participants in Study 1 obtained predominantly better performance results than those in Study 2, the clinicians of Study 2 reported higher scores for auditory display, suggesting that such a novel method would garner high levels of acceptance by operating clinicians. With increased training, the performance levels of clinicians could hypothetically also reach those of novice users. In addition, the growing popularity of video gaming has shown positive effects on surgical task completion time and error rate [37]. In our results, average task completion times for participants who play video games more than a few times per month were much lower (9.27 s per sphere for gamers vs 16.40 s for nongamers), and error rates were slightly lower (1.81 mm per sphere for gamers vs 1.98 mm for nongamers).

Finally, in consultation with our collaborating clinicians, we have determined that for this type of scenario, the use of open, over-the-ear headphones would not present ergonomic or performance challenges. However, commercially available bone-conduction headphones, which do not transmit sound into the ear canal but rather through jaw and cheekbones, would allow a clinician to make use of the auditory display while still hearing all speech inside the operating room. Further evaluations must determine whether this would provide suitable playback and deliver equivalent benefits.

5. Conclusion

This work presents an auditory display method developed to aid a broad spectrum of image-guided medical navigation approaches and focuses on two specific use cases of transnasal continuum robot navigation.

The auditory display method has been shown to benefit instrument placement to reach targets within a simulated sphenoidal sinus scenario. User studies with both novice and medical participants showed that the auditory display provided significant improvements in both quantitative performance measures and qualitative usability measures when performing transnasal navigation tasks in the simulated environment.

At this stage of research, this work shows progress in investigation of the effect of auditory display on continuum robot placement using a simulated environment. Based on these promising results, further evaluations will aim to employ physical phantom models and real continuum robots. Furthermore, future work will focus on refining and expanding auditory display method. A hybrid method of synthesized tones and natural voice samples could provide more intuitive directional cues given by the virtual choir as well as more fine-grained navigation given by additional synthesized tones. In addition to determining optimal auditory display mappings, increased focus should be placed on the role of auditory display in the operating room, especially with regards to augmenting existing visual methods. Supplementing existing visual navigation aids, for example, with auditory depth cues or distance-based risk warnings could enhance interaction with the system. A crucial element of future work is the investigation of the effects of both auditory and haptic feedback on performance for guidance. Previous work has show that combining haptic and visual feedback can increase accuracy and reduce task completion time compared to either modality separately [21, 22]. Thus, we hypothesize that performance with a thoughtfully designed, multimodal application of auditory, haptic, and/or visual feedback could surpass those described in this work. In this work, we describe an auditory display method developed to support this type of navigation. The described auditory display for tunnel-like navigation aid could, however, also be used to guide tasks with fewer degrees of freedom, such as a liver resection line (as employed by Hansen *et al.* [14]), absolute distance to risk structures (as seen in Cho *et al.* [12]), or ureteroscopy guidance [25].

In summary, this work describes an auditory display method which can be applied to a wide range of clinical use cases involving image-guided navigation. We confirm our overall hypotheses that the addition of auditory display increases accuracy, efficiency, task completion time, and usability, and reduces cognitive workload for tubular continuum robot navigation tasks. It is clear that auditory display will not replace visual navigation methods that have been refined and successfully implemented in the surgical routine over many decades. However, auditory display could be employed in many instances during which the view of a patient or situs is compromised or when monitors are inconveniently placed.

Informed consent

Informed consent was obtained from all individual participants included in the study.

Acknowledgments

The study was supported by National Institutes of Health Grants P41 EB015902, P41 EB015898, R01EB014955, U24CA180918 and funded by the German Research Foundations Emmy Noether Programme under award BU 2935/1-1. This work was supported by the German Federal Ministry of Education and Research (BMBF).

References

1. H. B. Gilbert, D. C. Ruckert and R. Webster III, Concentric tube robots: The state of the art and future directions, *Spring. Tracts Adv. Robot.* **14**(114) (2015) 253–269.
2. J. Burgner, D. C. Rucker, H. B. Gilbert, P. J. Swaney, P. Russell, K. D. Weaver and R. Webster III, A telerobotic system for transnasal surgery, *IEEE/ASME Trans. Mechatron.* **19**(3) (2014) 996–1006.
3. K. Leibrandt, C. Bergeles and G. Z. Yang, On-line collision-free inverse kinematics with frictional active constraints for effective control of unstable concentric tube robots, in *2015 IEEE/RSJ Int. Conf. Intelligent Robots and Systems (IROS)*, pp. 3797–3804.
4. R. H. Taylor, A perspective on medical robotics, *Proc. IEEE*, **94**(9) (2006) 1652–1664.
5. J. Burgner-Kahrs, D. C. Rucker and H. Choset, Continuum robots for medical applications: A survey, *IEEE Trans. Robot.* **31**(6) (2016) 1261–1280.
6. J. Burgner, P. Swaney, R. Lathrop, K. Weaver and R. Webster 3rd, Debulking from within: A robotic steerable cannula for intracerebral hemorrhage evacuation, *IEEE Trans. Biomed. Eng.* **60**(9) (2013) 2567–2575.
7. A. H. Gosline, N. V. Vasilyev, E. J. Butler, C. Folk, A. Cohen, R. Chen, N. Lang, P. J. Del Nido and P. E. Dupont, Percutaneous intracardiac beating-heart surgery using metal MEMS tissue approximation tools, *Int. J. Robot. Res.* **31**(9) (2012) 1081–1093.
8. T. Anor, J. Madsen and P. Dupont, Algorithms for design of continuum robots using the concentric tubes approach: A neurosurgical example, in *IEEE Int. Conf. Robotics and Automation* (2011), pp. 667–673.
9. J. Burgner, D. Rucker, H. Gilbert, P. Swaney, P. Russell 3rd, K. Weaver and R. Webster, 3rd, A telerobotic system for transnasal surgery, *IEEE Trans. Mechatron.* **19**(3) (2014) 996–1006.
10. D. Black, J. Hettig, M. Luz, C. Hansen, R. Kikinis and H. Hahn, Auditory feedback to support image-guided medical needle placement, *J. Comput. Assist. Radiol. Surg.* **12**(9) (2017) 1655–1663.
11. F. Bork, B. Fuerst, A. Schneider, F. Pinto, C. Graumann and N. Navab, Auditory and visio-temporal distance coding for 3-dimensional perception in medical augmented reality, in *Proc. 2015 IEEE Int. Symp. Mixed and Augmented Reality* (2015) pp. 7–12.
12. B. Cho, M. Oka, N. Matsumoto, R. Ouchida, J. Hong and M. Hashizume, Warning navigation system using realtime safe region monitoring for otologic surgery, *J. Comput. Assisted Radiol. Surg.* **8**(3) (2013) 395–405.
13. B. Dixon, M. Daly, H. Chan, A. Vescan, I. Witterick and J. Irish, Augmented real-time navigation with critical structure proximity alerts for endoscopic skull base surgery, *Laryngoscope* **124**(4) (2014) 853–859.

14. C. Hansen, D. Black, C. Lange, F. Rieber, W. Lamad, M. Donati, K. Oldhafer and H. Hahn, Auditory support for resection guidance in navigated liver surgery, *J. Med. Robot. Comput. Assisted Surg.* **9**(1) (2013) 36–43.
15. P. Willems, H. Noordmans, J. van Overbeeke, M. Viergever, C. Tulleken and J. van der Sprenkel, The impact of auditory feedback on neuronavigation. *Acta Neurochirurg.* **147**(2) (2005) 167–173.
16. M. Kitagawa, D. Dokko, A. Okamura and D. Yuh, Effect of sensory substitution on suture-manipulation forces for robotic surgical systems, *Thoracic Cardiovasc. Surg.* **129**(1) (2005) 151–158.
17. D. Black, C. Hansen, A. Nabavi, R. Kikinis and H. Hahn, A survey of auditory display in image-guided interventions, *J. Comput. Assist. Radiol. Surg.* **12**(10) (2017) 1665–1676.
18. L. Kreuer, S. Lilge and J. Burgner-Kahrs, Entwicklung von Kontrollalgorithmen fuer die Teleoperation von tubulaeren Kontinuumsrobotern, in *Tagungsband der 16. Jahrestagung der Deutschen Gesellschaft fuer Computer- und Roboter-assistierte Chirurgie e.V.* (Hannover, 2017), pp. 79–84.
19. L. Torres, A. Kuntz, H. Gilbert, P. Swaney, R. Hendrick and R. Webster, 3rd, R. Alterovitz, A motion planning approach to automatic obstacle avoidance during concentric tube robot teleoperation, in *IEEE Int. Conf. Robotics and Automation* (2015) pp. 2361–2367.
20. G. Gras, K. Leibrandt, P. Wisanuvej, P. Giataganas, C. Seneci, M. Ye, J. Shang and G. Yang, Implicit gaze-assisted adaptive motion scaling for highly articulated instrument manipulation, in *IEEE Int. Conf. Robotics and Automation* (2017) pp. 4233–4239.
21. H. Culbertson, J. Walker, M. Raitor, A. Okamura and P. Stolka, Plane assist: The influence of haptics on ultrasound-based needle guidance, in *Int. Conf. Medical Image Computing and Computer-Assisted Intervention* (2016) pp. 370–377.
22. M. Abayazid, C. Pacchierotti, P. Moreiral, R. Alterovitz, D. Prattichizzo and S. Misral, Experimental evaluation of co-manipulated ultrasound- guided flexible needle steering, *Int. J. Med. Robot.* **12** (2) (2015) 219–230.
23. R. Sigrist, G. Rauter, R. Riener and P. Wolf, Augmented visual, auditory, haptic, and multimodal feedback in motor learning: A review, *Psychon. Bull. Rev.* **20**(1) (2012) 21–53.
24. F. Fischbach, J. Bunke, M. Thormann, G. Gaffke, K. Jungnickel, J. Smink and J. Ricke, MR-guided freehand biopsy of liver lesions with fast continuous imaging using a 1.0-T open MRI scanner: Experience in 50 patients, *Cardiovasc. Interv. Radiol.* **34**(1) (2011) 188–192.
25. B. Xavier, F. King, A. Hosny, D. Black, S. Pieper and J. Jayender, Mixed reality navigation for laparoscopic surgery, in *9th National Image-Guided Therapy Workshop* (Bethesda, MD, USA, 2017).
26. D. Rucker, B. Jones and R. Webster, 3rd, A geometrically exact model for externally loaded concentric tube continuum robots, *IEEE Trans. Robot.* **26**(5) (2010) 769–780.
27. 3D Systems Touch Haptic Device: https://de.3dsystems.com/haptics-devices/touch, accessed February 2018.
28. D. Rucker and R. Webster, 3rd, Computing Jacobians and Compliance Matrices for Externally Loaded Continuum Robots, in *IEEE Int. Conf. Robotics and Automation* (2011), pp. 945–950.
29. D. Meagher, Geometric modeling using octree encoding, *Comput. Graph. Image Process.* **19**(2) (1982) 129–147.
30. M. Puckette, Pure data: Another integrated computer music environment, in *Second Intercollege Computer Music Concerts* (Tachikawa, Japan, 1996), pp. 37–41.
31. Freeverb∼: https://puredata.info/downloads/freeverb, accessed February 2018.
32. International Organization of Standards, ISO/IEC TR 9126-4:2004 Software engineering – Product quality – Part 4: Quality in use metrics. Geneva, Switzerland, 2004.
33. J. Byers, A. Bittner and S. Hill, Traditional and raw task load index (TLX) correlations: Are paired comparisons necessary?, in *Advances in Industrial Ergonomics and Safety* (Taylor and Francis, London), pp. 481–485.
34. S. Hart, NASA-Task Load Index (NASA-TLX); 20 Years Later, in *Human Factors and Ergonomics Society 50th Annual Meeting* (2006), pp. 904–908.
35. J. Van der Laan, A. Heino and D. de Waard, A simple procedure for the assessment of acceptance of advanced transport telematics, *Transp. Res. C, Emerging Technol.* **5**(1) (1997) 1–10.
36. R Core Team, R: A language and environment for statistical computing. R Foundation for Statistical Computing, Vienna, Austria: http://www.R-project.org/, accessed July 2018.
37. J. C. Rosser Jr., P. Lynch, L. Cuddihy, D. Gentile, J. Klonsky and R. Merrell, The impact of video games on training surgeons in the 21st century, *J. Arch. Surg.* **142**(2) (2007) 181–186.
38. S. Siegal, *Nonparametric Statistics for the Behavioral Sciences* (McGraw-hill, 1956).

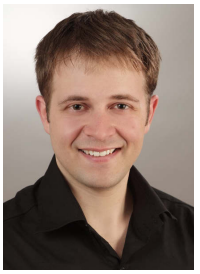

David Black is a researcher at the University of Bremen, Germany and the Fraunhofer Institute for Digital Medicine MEVIS in Bremen, Germany. He completed his PhD in computer science at Jacobs University in Bremen, Germany. In addition, has a background in sound design, electroacoustic music composition, and digital media. He currently investigates approaches for using auditory display in image-guided medicine and has published several eminent and ground-breaking articles on the topic.

Sven Lilge is a research assistant/PhD student at the Laboratory for Continuum Robotics, Leibniz University Hanover, Germany since 2017. He has a Master Degree in Electrical Engineering and Information Technology. His research focuses on the human–machine interaction for continuum robots.

Carolin Fellman has been a research assistant at the Laboratory for Continuum Robotics, Leibniz University Hanover, Germany since 2013. She has a Master degree in Systems Engineering and her main research focus lies on motion planning and human–machine interfaces for continuum robots in surgical applications.

Anke V. Reinschluessel is a research assistant/PhD student at the Digital Media Lab led by Professor Rainer Malaka at the University of Bremen, Germany since 2016. She has Bachelor Degree in Cognitive Science and Master Degree in Human–Computer Interaction. Her research focuses on innovative multimodal user interfaces.

Lars Kreuer was a student research assistant at the Laboratory for Continuum Robotics, Leibniz University Hanover from 2016 to 2017. His master's thesis focused on using virtual fixtures in the context of concentric tube continuum robot teleoperation.

Arya Nabavi is a neurosurgeon. His research centers around using computer- and robot-assisted surgery and intraoperative MRI to improve surgical treatment of his patients.

Horst K. Hahn studied Physics in Bayreuth, Toulouse, and Heidelberg. He is a director of Fraunhofer MEVIS, Institute for Medical Image Computing, and Professor of Medical Imaging at Jacobs University, both located in Bremen, Germany. His scientific and technological work addresses the digital transformation of medicine on the basis of multidisciplinary data integration and modern machine learning methods. In face of the rapidly advancing specialization of modern medicine with ever-increasing amounts of data and at the same time increasing cost pressure in the overall health system, his research aims at a sustained increase in efficiency and at the same time raising the quality and safety of both diagnostic and therapeutic processes.

Ron Kikinis is the founding Director of the Surgical Planning Laboratory, Department of Radiology, Brigham and Women's Hospital, Harvard Medical School, Boston, MA, and a Professor of Radiology at Harvard Medical School. This laboratory was founded in 1990. Before joining Brigham & Women's Hospital in 1988, he trained as a resident in Radiology at the University Hospital in Zurich, and as a Researcher in Computer Vision at the ETH in Zurich, Switzerland. He received his M.D. degree from the University of Zurich, Switzerland, in 1982. In 2004, he was appointed as Professor of Radiology at Harvard Medical School. In 2009, he was the inaugural recipient of the MICCAI Society "Enduring Impact Award". On February 24, 2010, he was appointed as the Robert Greenes Distinguished Director of Biomedical Informatics in the Department of Radiology at Brigham and Women's Hospital. On January 1, 2014, he was appointed "Institutsleiter" of Fraunhofer MEVIS and Professor of Medical Image Computing at the University of Bremen. Since then, he commutes every two months between Bremen and Boston.

Jessica Burgner-Kahrs received the Diploma degree in Computer Science from Universtaet Karlsruhe, Karlsruhe, Germany, in 2006 and the doctoral degree in Computer Science (Dr.-Ing.) from Karlsruhe Institute of Technology, Karlsruhe. From 2010 to 2012, she was with the Mechanical Engineering Department, Vanderbilt University, Nashville, TN, USA, as a Research Associate. In 2013, she joined Leibniz Universitaet Hannover, Hannover, Germany. She is an Associate Professor of Mechanical Engineering and Director of the Laboratory for Continuum Robotics. Dr. Burgner-Kahrs was awarded at the Emmy Noether Program of the German Research Foundation (DFG) in April 2013 and received the Heinz Maier-Leibnitz-Prize in 2015.